Laboratory Investigation (2019) 99:1376–1388
https://doi.org/10.1038/s41374-019-0259-0

ARTICLE

Dynamic signature of lymphangiogenesis during acute kidney injury and chronic kidney disease

Abolfazl Zarjou[1,2] · Laurence M. Black[1,2] · Subhashini Bolisetty[1,2] · Amie M. Traylor[1,2] · Sarah A. Bowhay[1,2] · Ming-Zhi Zhang[3,4] · Raymond C. Harris[3,5,6] · Anupam Agarwal[1,2,7]

Received: 17 January 2019 / Revised: 7 March 2019 / Accepted: 29 March 2019 / Published online: 24 April 2019

Abstract

Acute kidney injury (AKI) and chronic kidney disease (CKD) are interconnected syndromes with significant attributable morbidity and mortality. The disturbing trend of increasing incidence and prevalence of these clinical disorders highlights the urgent need for better understanding of the underlying mechanisms that are involved in pathogenesis of these conditions. Lymphangiogenesis and its involvement in various inflammatory conditions is increasingly recognized while its role in AKI and CKD remains to be fully elucidated. Here, we studied lymphangiogenesis in three models of kidney injury. Our results demonstrate that the main ligands for lymphangiogenesis, VEGF-C and VEGF-D, are abundantly present in tubules at baseline conditions and the expression pattern of these ligands is significantly altered following injury. In addition, we show that both of these ligands increase in serum and urine post-injury and suggest that such increment may serve as novel urinary biomarkers of AKI as well as in progression of kidney disease. We also provide evidence that irrespective of the nature of initial insult, lymphangiogenic pathways are rapidly and robustly induced as evidenced by higher expression of lymphatic markers within the kidney.

Introduction

Acute kidney injury (AKI) remains a major cause of morbidity and mortality, developing in about 5–7% of hospitalized patients and impairing recovery in 15–25% of those in intensive care units [1–3]. Additionally, AKI is linked to the subsequent development of chronic kidney disease (CKD) [4–6]. Lack of significant progress in the development of therapeutic interventions that are directed at both AKI and CKD highlights the urgent need for further delineation of pathways involved in the pathogenesis of these clinical conditions.

Despite its recognition since the ancient Greeks, the lymphatic vasculature was nearly impossible to study until about three decades ago because it was almost indistinguishable from the blood vessels. However, several pioneering studies changed this paradigm and led to an enhanced understanding of the molecular mechanisms involved in the regulation of lymphangiogenesis (LA). Moreover, it is now evident that LA commonly occurs in various disease states. The discovery of selective hyperplasia of the lymphatic vasculature in the skin via overexpression of vascular endothelial growth factor-C (VEGF-C) is regarded as the first major development towards deciphering the lymphatic system [7]. This work also demonstrated that VEGF-C mainly exerts its function through VEGF-R3 (FLT-4), a tyrosine kinase receptor. This was followed by the discovery of several other markers that

Supplementary information The online version of this article (https://doi.org/10.1038/s41374-019-0259-0) contains supplementary material, which is available to authorized users.

✉ Anupam Agarwal
agarwal@uab.edu

1 Department of Medicine, University of Alabama at Birmingham, Birmingham, USA

2 Nephrology Research and Training Center, University of Alabama at Birmingham, Birmingham, AL 35294, USA

3 Department of Medicine, Vanderbilt University School of Medicine, Nashville, USA

4 Department of Cancer Biology, Vanderbilt University School of Medicine, Nashville, USA

5 Department of Molecular Physiology and Biophysics, Vanderbilt University School of Medicine, Nashville, TN, USA

6 Nashville Veterans Affairs Hospital, Nashville, TN, USA

7 Department of Veterans Affairs, Birmingham, AL, USA

are predominately expressed by lymphatic endothelial cells. These include mucin type transmembrane glycoprotein podoplanin [8], and lymphatic vessel endothelial hyaluronan receptor-1 (LYVE-1) [9]. Furthermore, prosper-orelated homeobox transcription factor-1 (Prox-1) was demonstrated as a specific and required regulator for lymphatic system development [10]. Collectively, these discoveries have enabled precise and more in depth studying of the development of lymphatics in both health and disease.

The classic functions of the lymphatic system include maintenance of tissue fluid homeostasis, lipid absorption, and immune surveillance [11]. However, numerous studies have now shown that the lymphatic system also plays a vital role in the process of inflammation, characterized by increased vascular permeability, excess fluid accumulation, debris buildup, as well as migration and activation of leukocytes [12]. While little is known about the association and correlation between kidney disease and lymphangiogenesis, the anatomical architecture of renal lymphatics under physiological circumstances has been well described. Renal lymph vessels enter and follow a similar path of branching to renal arteries and veins. Accordingly, under normal conditions very few lymphatic vessels are present in cortical and medullary interstitial space. The lymphatic capillaries play a crucial role by collecting and transporting interstitial fluid and macromolecules into lymphatic pre-collectors that follow the arcuate and interlobar vessels into hilar collector lymphatics that eventually drain into the thoracic duct that empties into the left subclavian vein [13, 14]. The functions of the lymphatic system are further accentuated during inflammation, which is a key component of AKI and the AKI to CKD transition. Inflammation induces LA through expression of VEGFs, particularly VEGF-C, VEGF-D, and their receptor VEGF-R3 [15–17]. It has been shown that there is a clear link between LA and a number of inflammatory diseases including tumor metastasis, chronic airway infection, psoriasis, rheumatoid arthritis, corneal injury, wound healing, Crohn's disease, transplant rejection, and inflammatory bowel disease [12, 18, 19].

There are very few studies on LA in kidney diseases (most recent findings reviewed by Yazdani and colleagues) [14] and no work to date on LA in the context of AKI. This gap in knowledge prompted us to examine the course of LA during AKI and CKD in three different models of kidney disease.

Materials and methods

Study approval

All procedures involving mice were performed in accordance with National Institutes of Health guidelines regarding the care and use of live animals and were reviewed and approved by the Institutional Animal Care and Use Committee of University of Alabama at Birmingham and Vanderbilt University.

Ischemia/reperfusion injury

Age matched male (9 weeks at the time of delivery and 10 weeks old at the time of surgery) C57BL/6 were purchased from Jackson Laboratory. Renal I/R injury was performed as described previously with minor modifications [20]. Briefly, mice (10–12-weeks-old males) were anesthetized with ketamine (100 mg/kg) and xylazine (10 mg/kg), and following incision, both renal pedicles were cross clamped for 20 min using an atraumatic vascular clamp (catalog #18055–05; Fine Science Tools, Foster City, CA). Immediate blanching of the kidney confirmed ischemic induction. Body temperature was maintained at 37 °C during surgery and ischemia time. Kidneys were inspected for color change within 1 min of clamp removal to ensure uniform reperfusion.

High dose (HD) and repeated low dose (RLD) cisplatin administration

Cisplatin was purchased from Sigma Aldrich (St. Louis, MO). For the high dose (HD) model, aged matched C57BL/6 male mice (10–12 weeks of age) were administered cisplatin (1.0 mg/ml solution in sterile normal saline) at 20 mg/kg body weight by a single intraperitoneal injection as previously described [21, 22]. These animals were sacrificed 72 h after injection. For the repeated low dose (RLD) model, age-matched C57BL/6 male mice (10–12 weeks of age) were briefly anesthetized with isoflurane, and 9 mg/kg body wt cisplatin (1.0 mg/ml solution in sterile 0.9% saline) were administered intraperitoneally once a week for 4 week, adapted from Sharp et al. and Black et al. [23, 24].

Diphtheria toxin (DT) administration and AKI

All the details regarding generation of transgenic mice that selectively express the human DT-receptor in proximal tubules, dose and route of DT administration to induce AKI, renal function and other information have been reported previously [25].

Renal function measurements

Serum creatinine levels were measured by liquid chromatography-tandem mass spectrometry at the University of Alabama at Birmingham-University of California, San Diego O'Brien Center for Acute Kidney Injury

Research bioanalytical core facility by previously described methods [26].

Western blot analysis

Tissues and cells were homogenized and protein was isolated, as described previously [22]. Briefly, kidneys and cells were lysed in lysis buffer (10 mM/l Tris·HCl, 5 mM/l EDTA, 150 mM/l NaCl, 10% Nonidet P-40, and 10% Triton-X) with protease (Sigma-Aldrich, St. Louis, MO) and phosphatase (Biotool, Houston, TX) inhibitors. Total protein was quantified with the bichinchoninic acid protein assay (ThermoFisher, Waltham, MA). Protein (50 µg) was resolved on 12% Tris-glycine SDS-PAGE and transferred to a PVDF membrane (EMB Millipore, Billerica, MA). Membranes were blocked according to manufacturer's protocol (5% nonfat dry milk in PBST) for 1 h and then incubated with a goat anti-VEGFR-3 antibody (R&D Systems, Minneapolis, MN; 1:200), a rabbit anti-VEGF-D antibody (Abcam, Cambridge, MA; 1:2500), a mouse anti-VEGF-C antibody (Santa Cruz Biotechnology, Dallas, TX; 1:1000), or a rabbit anti-Prox-1 antibody (Abcam, Cambridge, MA; 1:200) followed by a peroxidase-conjugated goat anti-rabbit (or mouse) IgG antibody or donkey anti-goat IgG antibody (Jackson ImmunoResearch Laboratories, West Grove, PA; 1:5000). Horseradish peroxidase activity was detected using enhanced chemiluminescence detection system (GE Healthcare) or KiwkQuant detection system (Kindle Biosciences, Greenwich, CT). The membrane was stripped and probed with anti-GAPDH antibody (Sigma-Aldrich, St. Louis, MO; 1:5000) to confirm loading and transfer. Densitometry analysis was performed and results were normalized to GAPDH expression.

Immunofluorescence microscopy

Immunofluorescence was performed as previously described [27]. Briefly, mouse kidneys were fixed with 10% formalin solution and embedded in paraffin. Five-micrometer-thick sections were prepared, deparaffinized with xylene, and then rehydrated in water through graded ethanol. Antigen retrieval was performed in a pressure cooker in Tris-EDTA solution, pH 9.0, for 20 min. Non-specific staining in the sections was blocked by incubation in a blocking buffer (1% bovine serum albumin, 0.2% nonfat dry milk, 300 µl of Triton-X in 100 ml of PBS) for 30 min. The sections were then incubated with a goat anti-VEGFR-3 antibody (R&D Systems, Minneapolis, MN; 1:50), a rabbit anti-VEGF-D antibody (Abcam, Cambridge, MA; 1:200), or a mouse anti-VEGF-C antibody (Santa Cruz Biotechnology, Houston, TX; 1:200) overnight at 4 °C. Incubation of rabbit or mouse or goat secondary antibodies conjugated to Alexa Fluor 488, Texas red or Alexa Fluor 594 (30 min at room temperature; 1:100–1:200 dilution, Thermo Fisher, Waltham, MA) was subsequently done after washes. As a control, unrelated appropriate IgG antibodies (Santa Cruz Biotechnology, Houston) were used, followed by species specific secondary antibodies conjugated to Alexa Fluor 488, Texas red or Alexa Fluor 594, under the same conditions. The images were taken by Leica DMIRB epifluorescence microscope (Leica Microsystems, IL, USA) using Image PRO 5.1 software (Media Cybernetics, Inc, MD, USA) or a Leica TCS SP5 confocal microscope (Leica Microsystems) Images were captured on a BZ-X700 All-In-One Fluorescence Microscope (Keyence, Istasca, IL).

To quantify the number of VEGF-R3 positive vessels each kidney section obtained from one individual mouse was carefully evaluated under 20× magnification and the numbers were recorded for each section and data presented as number of VEGF-R3 vessels/section.

Picrosirius red stain

Kidneys were fixed in 10% neutral buffered formalin for 24 h then embedded in paraffin. Tissues were stained with periodic acid-Schiff hematoxylin using standard protocols. Fibrosis was visualized and measured using picrosirius red (PSR). Sections were deparaffinized in xylene washes and rehydrated, incubated in PSR for 1 h, washed in acidified water, and dehydrated. Sections were mounted in a resinous medium. All images were acquired on a BZ-X700 All-In-One Fluorescence Microscope (Keyence, Istasca, IL). Four to six random fields were selected from each section for digital quantification ($n = 3$/group). Images were acquired at 10× magnification. Percent area positive and intensity (integrated density) of PSR stain were measured using the "Triangle" autothreshold method in FIJI version 1.51n. Color, brightness, and contrast adjustments were made in an identical manner for matched sections.

Quantification of mRNA expression

Gene expression analysis was performed, as previously described [22]. Briefly, total RNA was isolated from tissues using TRIzol (Thermo Fisher Scientific, Waltham, MA). Quantitative real-time polymerase chain reaction (RT-PCR) was performed using SYBR Green Master Mix (Thermo Fisher, Waltham, MA). Reactions were performed in triplicate and monitored using melting curve analysis. Relative mRNA expression was quantified using comparative threshold cycle method and normalized to GAPDH mRNA as an internal control. Primers used to detect the specific genes included the following: VEGF-R3, fwd: 5′-CCAT CGAGAGTCTGGACAGC-3′ and VEGF-R3, rev: 5′-CCG GGATGGTGGTCACATAG-3′; Prox-1, fwd: 5′-GAAGG GCTATCACCCAATCA-3′ and Prox-1, rev: 5′- TGAAC

CACTTGATGAGCTGC-3′; VEGF-C, fwd: 5′-AGACG GACACACATGGAGGT-3′ and VEGF-C, rev: 5′-AAAG ACTCAATGCATGCCAC-3′; VEGF-D, fwd: 5′-CTGC TCGGATCTGTTGTTCA-3′ and VEGF-D, rev: 5′- GTGT ACTTGGTGCAGGGCTT-3′; Lyve-1, fwd: 5′-GGCTTT GAGACTTGCAGCTATG-3′ and Lyve-1, rev: 5′-GCAG GAGTTAACCCAGGTGT-3′; podoplanin, fwd: 5′-CTCA AGCTTCAAGATGTGGACCGTGCCAGT-3′ and podoplanin, rev: 5′-GAGGAATTCGGGCGAGAACCTTCCA GAAAT-3′.

Cell culture

Bone marrow-derived macrophages (BMDM) were isolated from C57BL/6 mice (10–12 weeks of age), as previously described, with minor modifications [28]. Briefly, cells were flushed from bones and passed through a 40 µm cell strainer (Fisher Scientific, Pittsburgh, PA) and red blood cells were lysed in ACK lysis buffer (0.15 M NH4Cl, 10 mM KHCO3, 0.1 mM EDTA). Cells were plated in DMEM (Corning Cellgro, Corning, NY) containing 15% FBS (Atlanta Biologicals, Flowery Branch, GA), 1% non-essential amino acids (Gibco, Gaithersburg, MD), 30 ng/ml MCSF (Miltenyi Biotec, Auburn, CA), and 1% antibiotic/antimycotic (Thermo Fisher, Waltham, MA). BMDMs were cultured for 6 days before lysis and protein isolation. Primary proximal tubular cells (PTC) cultures were generated from the kidneys of C57BL/6 mice (10–12 weeks of age) using a previously described procedure [29]. Briefly, kidney cortices from mice were dissected from the medulla, sliced, minced, and filtered through a 70-µm cell strainer over a 50-ml conical tube with media (Renal Epithelial Cell Growth Medium; PromoCell, Heidelberg, Germany). The medium containing the tubules was centrifuged and plated on collagen-coated culture plates and then incubated for 72 h at 37 °C in 5% CO_2. Each experiment required PTC or BMDM generated from a single animal and cells were not passaged.

ELISA

ELISA analyses for VEGF-C (Cloud-Clone Corp., Atlanta, GA) and VEGF-D (My BioSource, San Diego, CA) were performed on serum or urine following the manufacturer's instructions. Urine creatinine was measured by LC-MS/MS [26]. VEGF-C data were expressed as nanograms per milliliter and VEGF-D data as picograms per milliliter. Urine data were normalized to urine creatinine and expressed as nanograms or picograms per milligram creatinine for VEGF-C and VEGF-D, respectively. Per manufactures' manual, both VEGF-C and VEGF-D ELISA kits are highly sensitive and specific with no cross-reactivity with other factors. The reported intra-assay and inter-assay variability for VEGF-C ELISA kit is reported at <10 and <12%, respectively. The reported intra-assay and inter-assay variability for VEGF-D ELISA kit is reported at <8 and <12%, respectively.

Statistical analysis

Data are represented as mean ±SEM. Unpaired two-tailed *t*-test was used for comparisons between two groups. ANOVA and Tukey's multiple comparisons tests were used for comparisons between more than two groups. *P* values less than 0.05 were considered significant. All analysis was performed using GraphPad Prism 7.

Results

Ischemia/reperfusion model to induce AKI and CKD

To investigate LA in the context of both AKI and CKD, we first used ischemia-reperfusion (I/R) as a well-established model of AKI and the subsequent development of CKD. Following I/R, renal function was assessed by measuring serum creatinine at 1, 3, 7, 14, and 28 days post injury and compared to baseline levels. As expected, serum creatinine was markedly elevated at 1 day post-I/R and gradually decreased towards baseline (Fig. 1a). We also assessed the extent of fibrosis and collagen deposition by picosiruis red staining. As shown in Fig. 1b, c, collagen deposition increased following injury and was highest by days 14 and 28.

I/R induced kidney injury stimulates dynamic changes in inducers and markers of lymphangiogenesis

We next determined the kidney mRNA levels of VEGF-C and VEGF-D, which are known to be central ligands in stimulation of LA. The levels of both these ligands significantly increased following injury. VEGF-C levels gradually increased over time and were significant at days 14 and 28. In contrast, VEGF-D levels were significantly higher on day 3 (Fig. 2). Other markers of LA including VEGF-R3, LYVE-1, and podoplanin showed a trend of increased expression compared to baseline at various timepoints (Fig. 2). However, significant variability among samples was noted, likely reflecting the scattered distribution of the lymphatics within the renal parenchymal tissue. In addition, Prox-1, the central transcription factor that is required for neo-LA, was significantly suppressed at the RNA level on day 3 post injury followed by a significant increase on day 14 (Fig. 2). These results mimic previous findings that investigated cardiac LA following myocardial infarction [30]. We then examined the renal protein

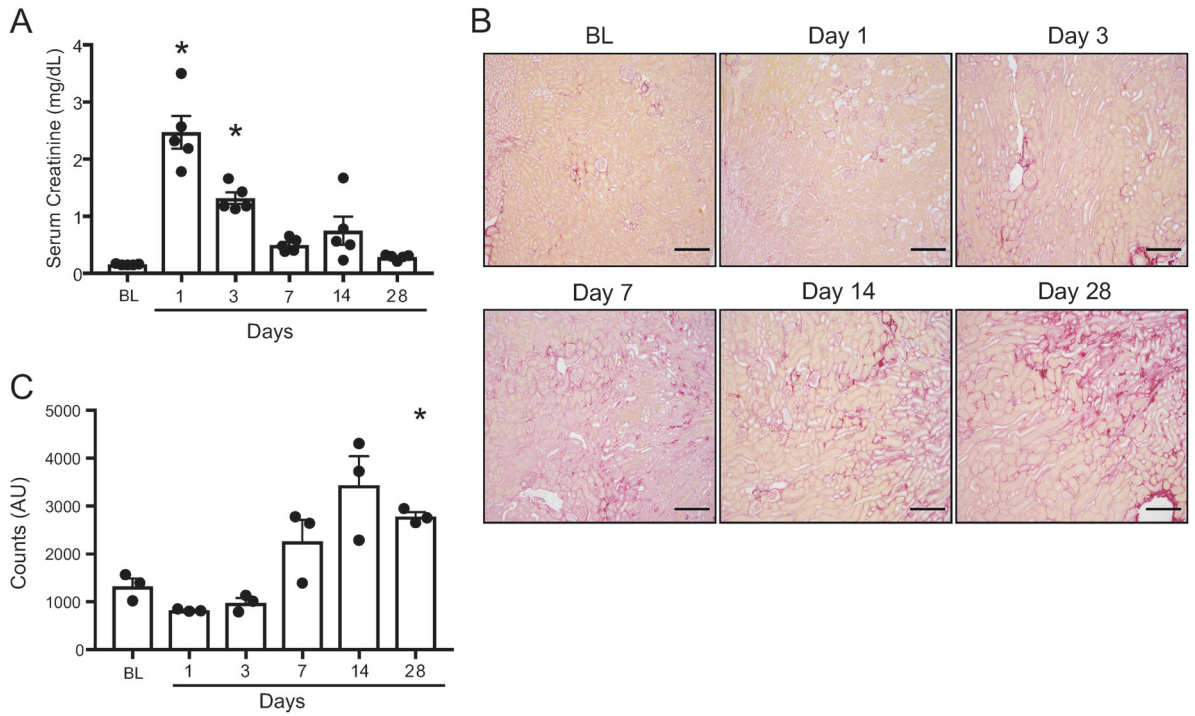

Fig. 1 Renal ischemia/reperfusion (I/R) induces kidney injury and subsequent fibrosis. **a** Serum creatinine levels were measured and expressed as milligrams/deciliter (mg/dL) at baseline and on days 1, 3, 7, 14, 28 following I/R. Data are expressed as means ± SEM; $^{*}P < 0.05$ vs. baseline. **b** Picrosirius red stain demonstrating collagen deposition at various time points following injury. **c** Quantification of collagen deposition by measuring intensity of picrosirius stain encompassing positive staining areas above threshold. Data are expressed as means ± SEM; $^{*}P < 0.05$ vs. baseline. Scale bar = 200 μm

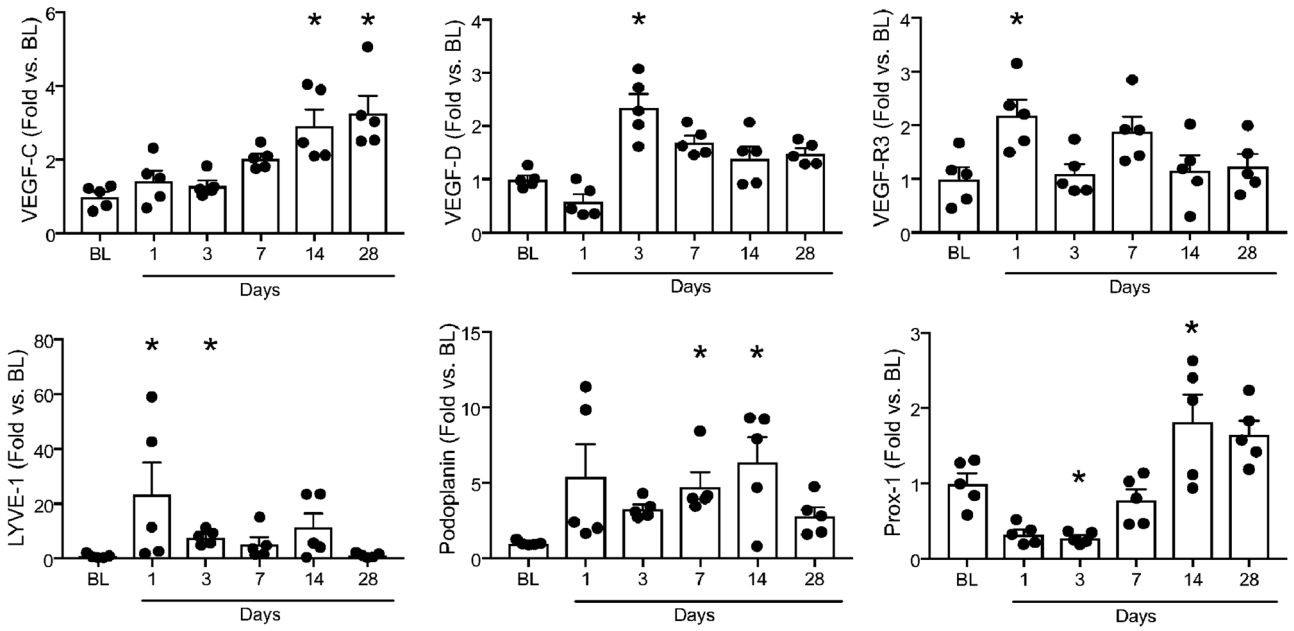

Fig. 2 I/R induces expression of ligands and markers involved in lymphangiogenesis (LA). Total RNA was isolated from kidneys at baseline and different time points after I/R mediated kidney injury and analyzed for the expression of VEGF-C, VEGF-D, VEGF-R3, LYVE-1, podoplanin, and prox-1. Results were normalized to GAPDH and expressed as fold change relative to baseline controls. Data are expressed as means ± SEM; $^{*}P < 0.05$ vs. baseline

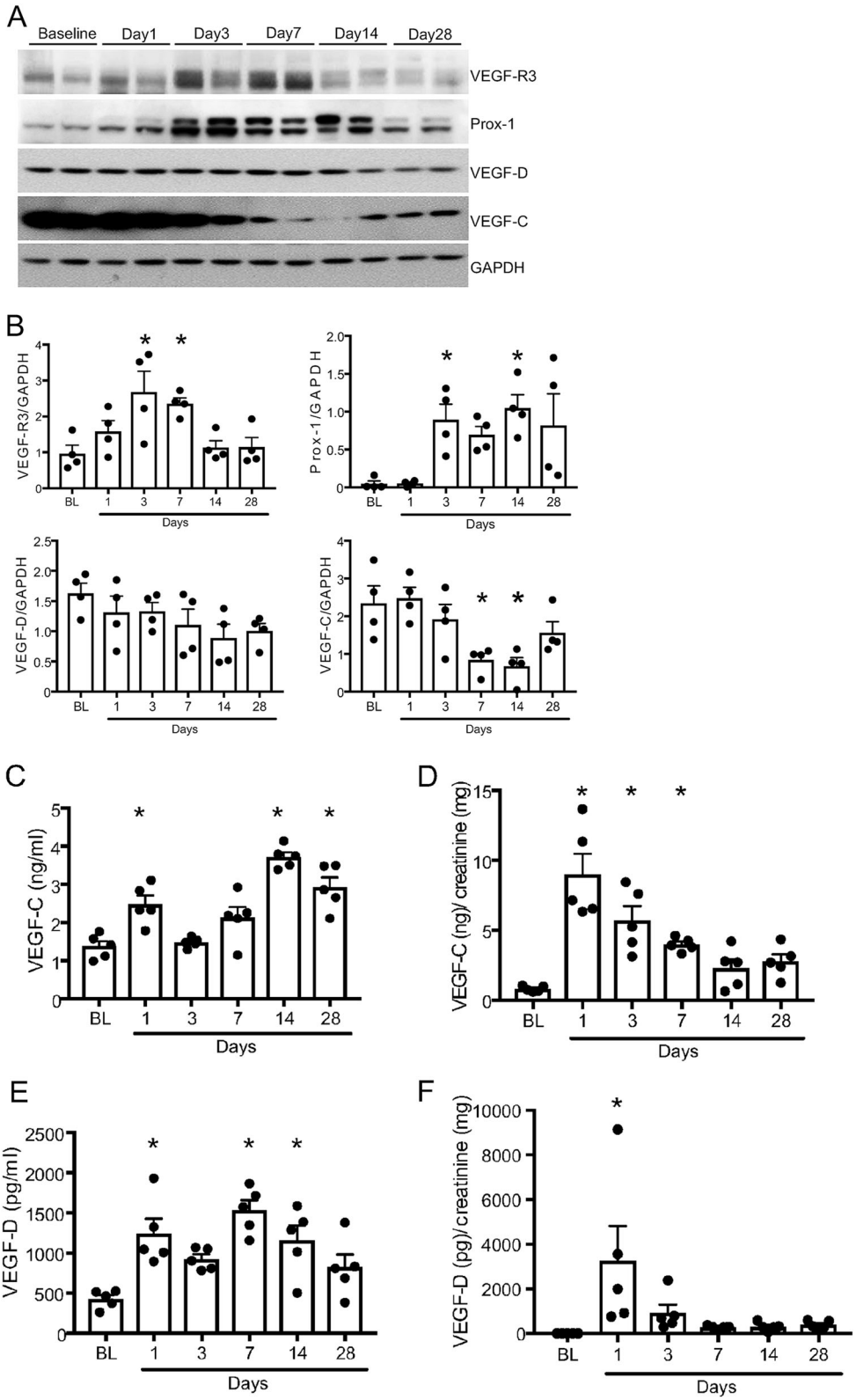

Fig. 3 Protein levels of LA ligands and markers are upregulated following I/R induced injury. **a** Protein expression level of VEGF-R3, Prox-1, VEGF-D, and VEGF-C was verified by Western blot. Blots were stripped and probed for GAPDH. **b** Expression of the indicated proteins in the kidneys was analyzed by densitometry, normalized to GAPDH, and expressed as mean ± SEM. *$P <$ 0.05 vs. baseline. **c**, **e** Serum was collected at indicated time points and levels of VEGF-C (**c**) and VEGF-D (**e**) were measured by ELISA and data expressed as nanogram per milliliter or picogram per milliliter, respectively. **d**, **f** Urine was collected at the time of sacrifice via bladder puncture and evaluated for levels of VEGF-C (**d**) and VEGF-D (**f**). Results were then normalized to urine creatinine levels and expressed as nanogram per milligram and picogram per milligram creatinine for VEGF-C and VEGF-D, respectively. Results expressed as mean ± SEM. *$P <$ 0.05 vs. baseline

expression of VEGF-C, VEGF-D, VEGF-R3 and Prox-1 by Western blotting. Renal expression of both VEGF-C and VEGF-D decreased over time while VEGF-R3 and Prox-1 increased following injury (Fig. 3a, b). Conversely, expression levels of VEGF-R3 and Prox-1 were significantly higher compared to baseline at day 3 (Fig. 3b).

The aforementioned results led us to hypothesize that the decrement in the level of parenchymal VEGF-C and

VEGF-D protein expression is reflective of their secretion into the interstitium, circulation, and/or urine. To confirm this, we performed ELISA to quantify serum and urinary levels of VEGF-C and VEGF-D following injury. Both VEGF-C and VEGF-D increased significantly in the serum post injury compared to baseline (Fig. 3c, e). Serum levels of VEGF-C were significantly higher on days 1, 14, and 28 and VEGF-D on days 1, 7, and 14 after injury. Interestingly, both VEGF-C and VEGF-D levels were significantly elevated in the urine following injury (Fig. 3d, f). These results indicate that the ligands required for induction of LA are available at baseline and rapidly secreted either through active secretory pathways or via direct release following injury to the cell.

Expression patterns of VEGF-C and VEGF-D change following I/R induced injury

>We next investigated the expression patterns of VEGF-C and VEGF-D at baseline and following I/R injury. We found that almost all tubules within the cortex and outer medulla were positive for both VEGF-C and VEGF-D expression which further corroborates that these ligands are pre-synthesized and secreted upon injury to promptly stimulate LA (Fig. 4a). At baseline, the expression was homogeneous in renal tubules and localized predominantly to the cytoplasmic compartment. Following injury, however, the pattern was altered. On day 1 following injury, VEGF-C was mainly localized on the basolateral surface while VEGF-D was found in the luminal portion of the tubules. It must be noted that our IgG controls demonstrate similar luminal staining on day 1 which likely represents non-specific staining of luminal cellular debris/casts. By day 7, several regenerating tubules were positive for both VEGF-C and VEGF-D with predominant basolateral staining. Such heterogeneous and patchy patterns of staining remained evident at days 14 and 28 (Fig. 4a). We hypothesize that the changes in distribution of both VEGF-C and VEGF-D expression may highlight the loss of polarity of tubular epithelial cells following injury and/or may reflect an active process of secretion into the interstitium and lumen. These speculations would require additional future studies for confirmation.

To visualize the dynamic proliferation of lymphatic vessels post injury, we stained kidney sections for VEGF-R3. Very few lymphatics were positive for VEGFR-3 at baseline and these were predominantly localized adjacent to the renal artery and vein at the hilum (data not shown). Starting on day 3, significantly higher numbers of VEGF-R3 positive lymphatic vessels were visualized that continued to increase until day 28 (Fig. 4b). These positively stained lymphatics were manually counted per section and results presented in Fig. 4c demonstrate progression of LA following I/R-induced injury.

Evaluation of lymphangiogenesis in cisplatin-induced nephrotoxicity

Since I/R entails clamping of the renal pedicle and includes the renal artery, vein and associated lymphatics that run parallel to them, we sought to corroborate that the robust LA observed following I/R is not merely due to mechanical damage inflicted during the clamping procedure. Hence, we utilized another well-established model of kidney injury induced by the administration of cisplatin in the context of both AKI and CKD. To this end a single injection of 20 mg/kg of cisplatin was used to induce AKI (high dose, HD), while repeated dosing of 9 mg/kg of cisplatin was administered once a week for 4 weeks to induce CKD (repeated low dose, RLD) as previously reported [23, 24]. For the AKI studies, tissues were harvested at 72 h post injury, while CKD studies were terminated at 28 days. To investigate the expression pattern of ligands required in cisplatin nephrotoxicity, we stained kidneys with VEGF-C and VEGF-D following cisplatin and compared them to baseline (Fig. 5a). Such comparison (although less prominent when compared to I/R) revealed more basolateral staining of VEGF-C in both AKI and CKD models. In contrast, high dose cisplatin led to increase in VEGF-D luminal staining. Moreover, injury resulted in a less uniform pattern of expression with tubules demonstrating variable intensity that likely reveals replenishing stores and regeneration following injury (Fig. 5a). We next examined the serum and urinary levels of major ligands of LA, VEGF-C, and VEGF-D by ELISA. As shown in Fig. 6a–d levels of both VEGF-C and VEGF-D were significantly higher in serum and urine in the repeated low dose cisplatin model. Serum VEGF-D levels however were not significantly different between high dose cisplatin and baseline (Fig. 6c). Furthermore, we did not detect any urinary VEGF-D at baseline (Fig. 6d).

To quantify and better understand the progression of LA following cisplatin nephrotoxicity, we examined VEGF-R3 expression and found that at baseline kidneys displayed few lymphatics, which were confined to the hilum. However, cisplatin induced robust LA as evidenced by the number of new vessels positive for VEGF-R3 in both high dose and repeated low dose groups (Fig. 7a). These positive vessels were counted per section and the quantified results are shown in Fig. 7b.

Induction of lymphangiogenesis in transgenic mice expressing human diphtheria toxin (DT) receptor in proximal tubules

While many mammals are sensitive to diphtheria toxin (DT), rodents are about 100 times more resistant, since DT does not bind to their heparin-binding EGF-like growth factor (HB-EGF) which is also the DT-receptor [31]. To

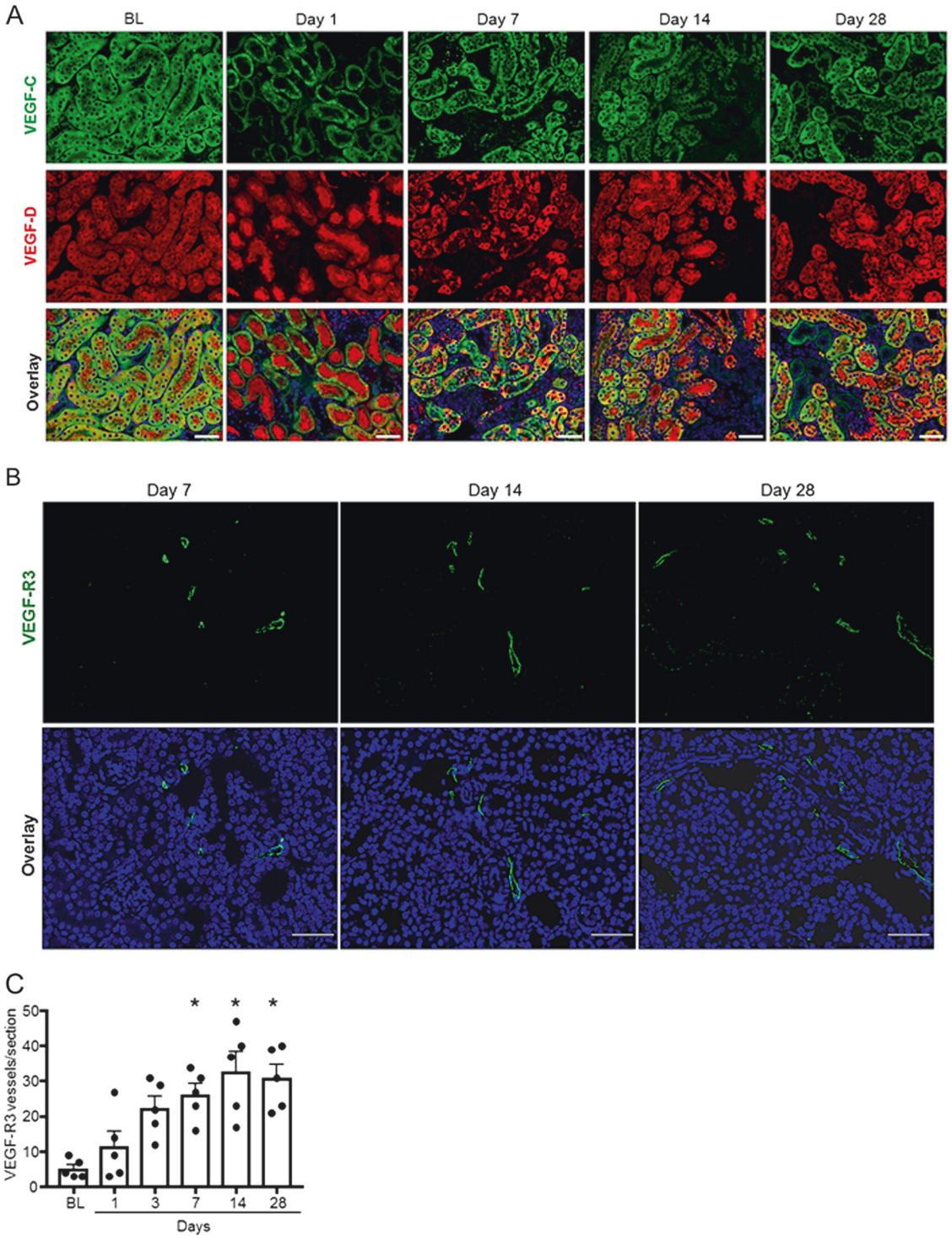

Fig. 4 I/R mediated injury changes the pattern of VEGF-C and VEGF-D expression and induces expression of VEGF-R3. **a** Mice were sacrificed at indicated time points and kidney sections were prepared and immunofluorescence assays were performed using anti-VEGF-C and anti-VEGF-D antibodies to determine the pattern of expression of these proteins. DAPI was used to stain nuclei. Images are representative of five independent experiments. Scale bar = 50 µm. **b** Kidneys sections were stained using anti-VEGF-R3 antibody. For better demonstration only the indicated time-points are shown. Scale bar = 50 µm. **c** Quantification of VEGF-R3 positive vessels was performed as described in methods. $^{*}P < 0.05$ vs. baseline

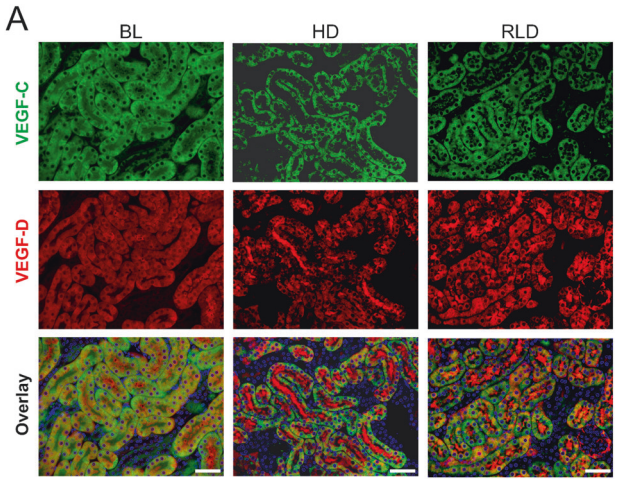

Fig. 5 Cisplatin induced nephrotoxicity alters tubular VEGF-C and VEGF-D expression pattern. **a** As described in methods section, mice were sacrificed at 3 days post HD and 28 days following RLD cisplatin administration. Kidney sections were prepared and immunofluorescence staining was performed using anti-VEGF-C and anti-VEGF-D antibodies. Images are representative of five independent experiments. Scale bar = 50 μm

further validate our initial findings, we next took advantage of a novel model of AKI in which transgenic mice express DT-receptor in proximal tubules [25]. Administration of DT results in marked elevation of BUN and apoptosis in these mice as previously reported [25]. Despite the different approach to induce AKI, both VEGF-C and VEGF-D expression within tubules closely resembled I/R and cisplatin induced kidney injury (Fig. 8a). Accordingly, significant basolateral staining for these ligands was observed in DT treated mice compared to baseline. This model did not reveal significant luminal VEGF-D staining which may be a result of the time of sacrifice which occurred following 8 days of DT administration. Additionally, we found significantly higher number of VEGF-R3 positive lymphatic vessels in DT treated mice compared to baseline that again highlights robust induction of renal LA irrespective of mode of kidney injury (Fig. 8b, c).

Tubules contribute to both VEGF-C and VEGF-D production while macrophages only express VEGF-C

It has been previously shown that both macrophages and renal tubules express VEGF-C that likely presents a major source of this ligand during injury associated LA. Here, we cultured proximal tubules (PTC) and bone marrow derived macrophages (Mφ) and examined their expression of these ligands. As shown by Western blotting in Fig. 9a, it is evident that while both of these cell types robustly express VEGF-C at basal conditions, only PTC contribute to VEGF-D production. We confirmed these findings by staining kidneys with DT-induced injury as well as from spleens from mice at baseline conditions (Fig. 9b). It must be noted that the very intense staining of VEGF-C in renal Mφ required us to decrease the intensity of staining to better depict these Mφ at expense of tubules.

Discussion

The results of this work demonstrate that the main ligands involved in LA, VEGF-C, and VEGF-D, are abundantly present in renal tubules at baseline and are secreted following injury. Lymphatic vessel formation is robustly induced following kidney injury and such induction is independent of the nature of insult. Our results also indicate that while both macrophages and renal tubules actively participate in secretion of VEGF-C and its subsequent contribution towards LA, VEGF-D is only produced by renal tubular cells and not macrophages. In addition, we demonstrate significantly higher urinary levels of both VEGF-C and VEGF-D following injury, suggesting that these factors may serve as biomarkers of LA in the setting of kidney injury. The observed changes in the staining pattern, expression of both mRNA and protein levels following injury substantiates the pivotal relationship between induction of LA in response to injury. However, future mechanistic studies are required to decipher whether such changes occur at the transcriptional, post-transcriptional, or post-translational level.

Inflammation induced LA could be considered an adaptive and beneficial response following injury as it would aid in clearance of debris, removal of pro-inflammatory cytokines, migration of regulatory T cells, and drainage of excess fluid. In contrast, LA during inflammation may also be regarded as a potentially harmful response since it could facilitate in the migration of leukocytes to the site of injury with subsequent exacerbation of inflammation. There is also evidence indicating that lymphatic endothelial cells can secrete cytokines to maintain the inflammatory environment. Inflammation induced LA is beneficial in certain conditions such as myocardial infarction [30], polycystic kidney disease [32], lung transplantation [33], and others [14]. However, LA can also be harmful in the setting of corneal transplantation [34, 35], diabetes [36, 37], and tumor metastasis (reviewed in the ref. [38, 39]).

Very little is currently known about LA in the pathophysiology of kidney diseases, particularly in the context of AKI and CKD. However, there have been several recent studies on LA in the setting of unilateral ureteral obstruction (UUO) that have shed some light on this process [40–43]. These studies revealed an increase in the number of lymphatic vessels in the kidney after UUO. LA was promoted in the kidneys via increased VEGF-C and VEGF-D protein expression stimulated at least in part by

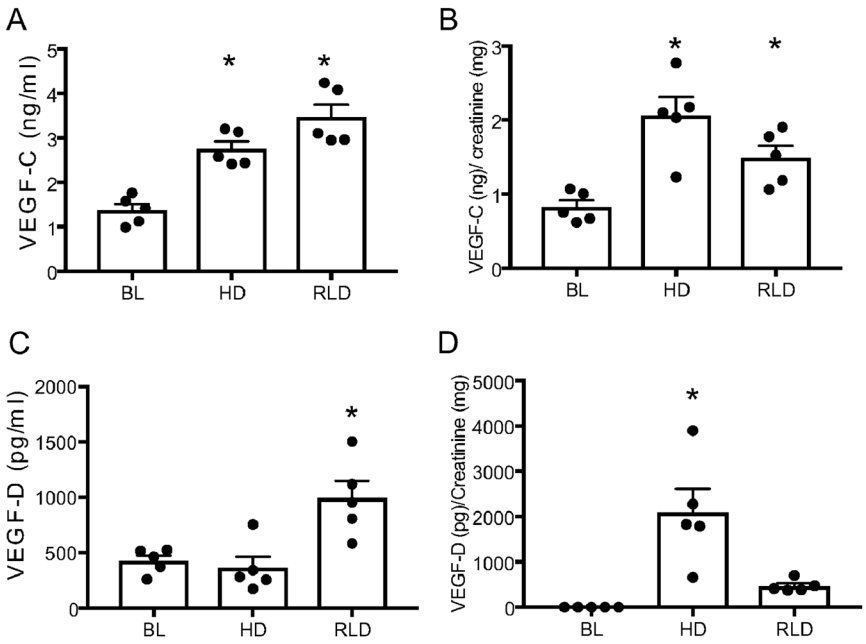

Fig. 6 Serum and urinary levels of VEGF-C and VEGF-D increase following cisplatin injury. **a**, **c** Mice were sacrificed at 3 days post HD and 28 days post RLD cisplatin administration. VEGF-C (**a**) and VEGF-D (**c**) levels in the serum were measured by ELISA and expressed as nanogram per milliliter and picogram per milliliter, respectively. $^{*}P < 0.05$ vs. baseline. **b**, **d** Urine was collected via bladder puncture at the time of sacrifice and ELISA was used to measure VEGF-C and VEGF-D levels. Results were then normalized to urine creatinine levels and expressed as nanogram per milligram and picogram per milligram creatinine for VEGF-C and VEGF-D, respectively. Results expressed as mean ± SEM. $^{*}P < 0.05$ vs. baseline

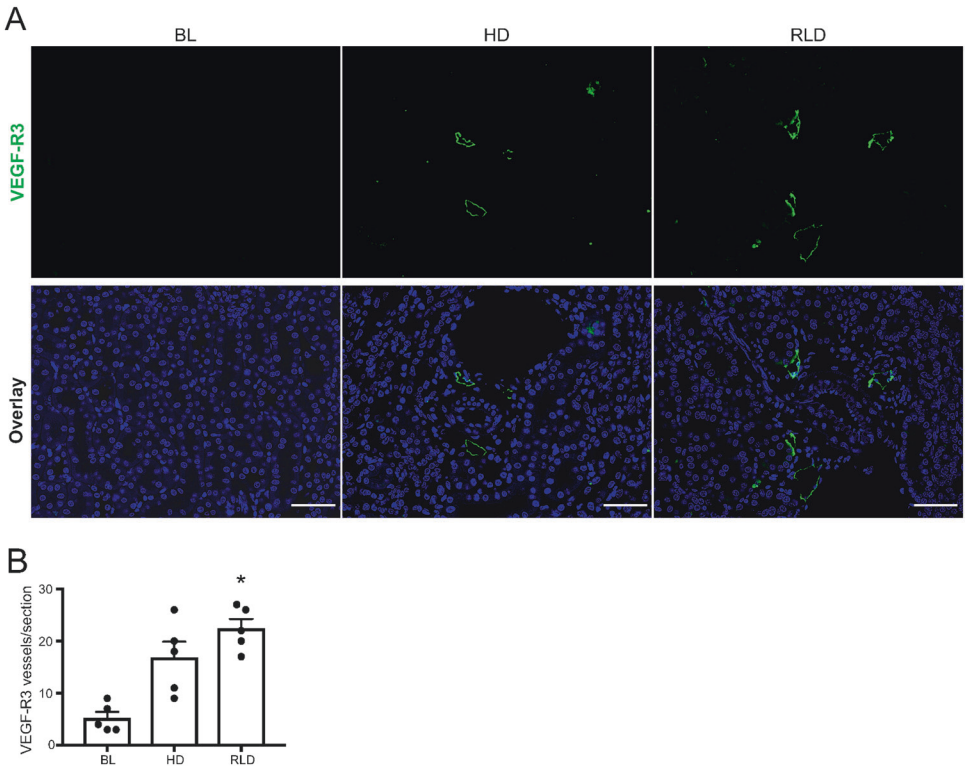

Fig. 7 VEGF-R3 expression increases in response to cisplatin nephrotoxicity. **a** Kidney sections at 3 days post HD and 28 days post RLD administration were stained with anti-VEGF-R3 antibody as described in methods section. Images are representative of five independent experiments. Scale bar = 50 µm. **b** Results demonstrate quantification of number of VEGF-R3 positive vessels/kidney section. Results expressed as mean ± SEM. $^{*}P < 0.05$ vs. baseline

TGF-β [42, 43]. While these studies have provided important insights regarding the mechanisms involved in renal LA, utilization of the UUO model may not be the ideal model to study these changes. This is particularly true when considering the role of lymphatics in fluid reabsorption and the fact that UUO leads to significant

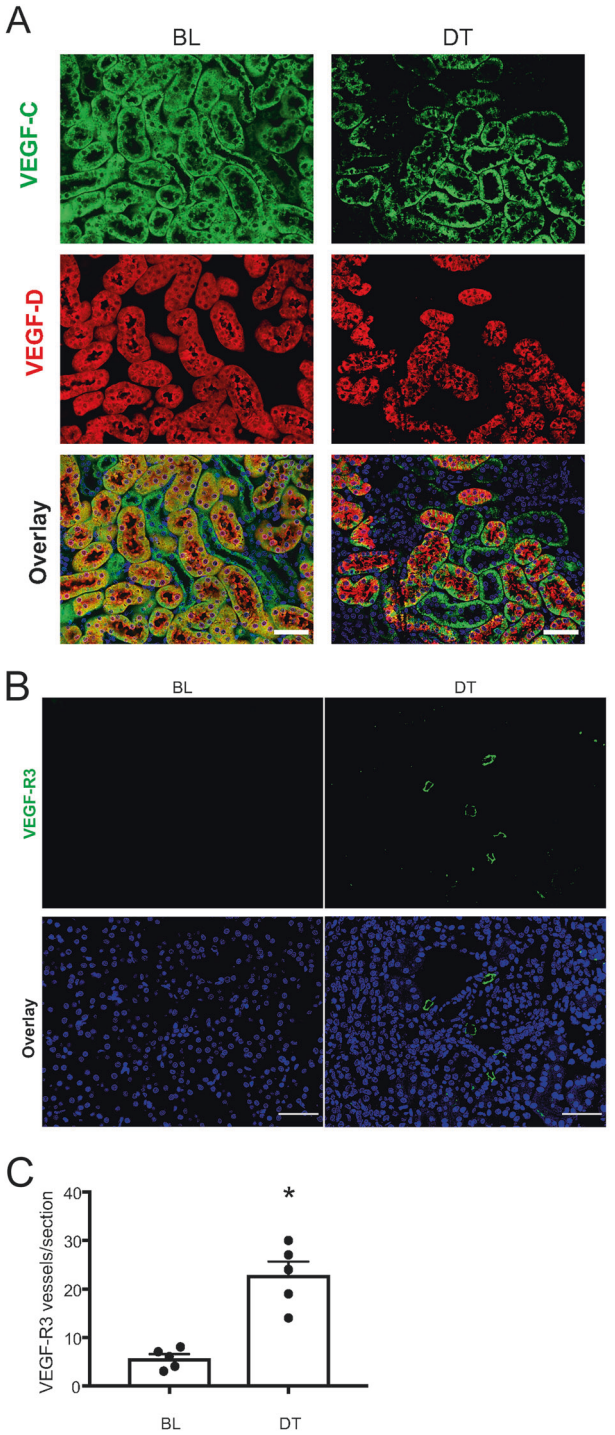

Fig. 8 DT induced proximal tubular injury affects expression of LA ligands and leads to induction of LA. **a** DT was administered to transgenic mice with selective expression of DT-receptor in proximal tubules and kidneys were harvested. Kidney sections were prepared and immunofluorescence staining was performed using anti-VEGF-C and anti-VEGF-D antibodies. DAPI was used to stain the nuclei. Images are representative of at least five independent experiments. Scale bar = 50 µm. **b** Kidney sections were stained with anti-VEGF-R3 antibody and nuclei were stained with DAPI. **c** Each stained kidney section was carefully evaluated to quantify the number of lymphatic vessels staining positive for VEGF-R3 and data was expressed as VEGF-R3 vessels per section. Images are representative of at least five independent experiments. Scale bar = 50 µm. Results expressed as mean ± SEM. $*P < 0.05$

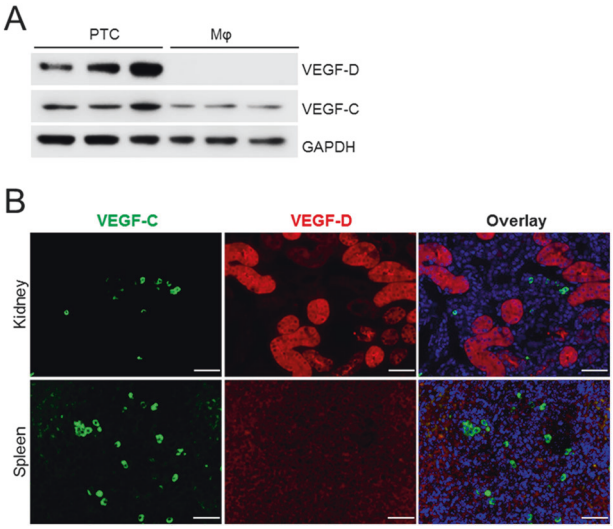

Fig. 9 Tubular cells are major source of VEGF-D while both macrophages and tubules contribute to VEGF-C production. **a** PTC and BMDM were harvested and their proteins were examined for VEGF-C and VEGF-D content via Western blotting. **b** Spleen and kidneys were stained for VEGF-C and VEGF-D. Immunofluorescence staining reveals macrophages that only express VEGF-C and renal tubules that express both VEGF-C and VEGF-D. Images are representative three independent experiments. Scale bar = 50 µm

urinary retention, hence confounding the precise nature of the initiating and maintaining factors leading to LA. Other studies have also implicated LA in renal transplant rejection. One study showed that nearly all end stage renal allografts had increased lymphatic vessel density likely contributing to the chronic renal allograft failure [44]. In addition, rat models of kidney allograft rejection show improved outcomes when LA is blocked after transplantation [45]. Inflammation induced LA has also been shown to play a role in the pathogenesis of diabetic kidney disease [14] and renal cancer [46, 47]. Lymphatic drainage and lymphatic contents from the injured kidney arriving at the systemic circulation and regional lymph nodes may provide a hitherto unrecognized pathway whereby the injured kidney may elicit adverse distant effects on organs such as heart, lungs, and brain, especially as the morbidity and mortality of AKI result largely from adverse effects on these distant, vital organs. Such distant cross-talk may be mediated via increased levels of circulating ligands promoting LA (VEGF-C and VEFG-D). Hence, it would be interesting for future studies to examine potentially increased LA in other major organs following AKI or during CKD.

To provide a more comprehensive understanding of the mediators and processes that orchestrate LA during kidney injury, our studies first focused on the initiation and progression of LA in I/R induced kidney injury. As demonstrated, we found upregulation of lymphatic markers and secretion of both VEGF-C and VEGF-D in serum and urine post-injury. An interesting aspect of these findings is the marked elevation of both VEGF-C and VEGF-D in urine samples of mice with I/R mediated injury and cisplatin nephrotoxicity. We postulate that this increase may be due to release of these ligands either through an active secretion process or merely the result of the breakdown of cellular barriers. While VEGF has previously been shown to be a potentially reliable urinary biomarker of AKI [48], to the best of our knowledge this is the first description of specific isoforms VEGF-C and VEGF-D in this context. These results may provide not only a novel biomarker of injury but will also offer a window into the dynamics of renal LA during injury.

To eliminate mechanical injury to the lymphatics due to clamping and subsequent injury to the main lymphatic vessels that enter the renal hilum during the ischemia phase, we were prompted to investigate LA during cisplatin nephrotoxicity. We found that similar to I/R mediated injury, cisplatin nephrotoxicity resulted in increase of urinary and serum VEGF-C and VEGF-D (although VEGF-D was only significantly higher in low-dose group). Such discrepancies in VEGF-D secretion may be a function of time (AKI vs. CKD) as well as severity of injury. Moreover, expression of VEGF-R3, used as a marker of LA, was significantly higher in both low and high dose cisplatin groups. We were also able to corroborate these findings in a model of DT-induced selective injury to the renal proximal tubule that has previously been described [25]. While our findings demonstrate robust induction of renal LA independent of the mode of injury, we acknowledge that future studies are required to determine the functional significance of LA in the setting of AKI and CKD and provide additional mechanistic insights. As alluded to earlier, the currently existing literature describing LA during kidney injury only involves the role of LA in UUO models. However, the essential contributing role of lymphatics in interstitial fluid reabsorption is a major limiting factor in full interpretation of these findings in the context of AKI and CKD where UUO is followed by marked parenchymal swelling and interstitial edema. Therefore, despite limitations in the context of functional significance, our findings provide important novel information that identifies neo-LA as an integral ensuing component of kidney injury that occurs irrespective of mode of injury. Whether LA would be an adaptive or maladaptive response to injury and inflammation during AKI and CKD would be a subject of future investigation.

In conclusion, we provide evidence that LA is induced during AKI and CKD. These results will likely provide a strong foundation to better study the lymphatic network in renal pathologies. We propose that timely targeting of this delicate and well-regulated pathway will allow future therapeutics to challenge AKI, interstitial fibrosis and ultimately prevent CKD.

Acknowledgements We appreciate the technical assistance of Kayla McCullough and Yanlin Jiang. This work was supported by NIH grants (1K08HL140294 to A. Zarjou, 5K01DK103931 to S. Bolisetty, 1T32DK116672 to L.M. Black, DK062794, DK95785, and DK114809 to R. Harris and M. Zhang), VA Merit Award 1I01BX004047 to A. Agarwal, T32 GM 109780 to S.A. Bowhay, the core resource of the UAB-UCSD O'Brien Center (P30 DK079337 to A. Agarwal).

Compliance with ethical standards

Conflict of interest The authors declare that they have no conflict of interest.

References

1. Mehta RL, Pascual MT, Soroko S, et al. Spectrum of acute renal failure in the intensive care unit: the PICARD experience. Kidney Int. 2004;66:1613–21.
2. Zarjou A, Sanders PW, Mehta RL, et al. Enabling innovative translational research in acute kidney injury. Clin Transl Sci. 2012;5:93–101.
3. de Caestecker M, Harris R. Translating knowledge into therapy for acute kidney injury. Semin Nephrol. 2018;38:88–97.
4. Chawla LS, Eggers PW, Star RA, et al. Acute kidney injury and chronic kidney disease as interconnected syndromes. N Engl J Med. 2014;371:58–66.
5. Chawla LS, Kimmel PL. Acute kidney injury and chronic kidney disease: an integrated clinical syndrome. Kidney Int. 2012;82:516–24.
6. Waikar SS, Liu KD, Chertow GM. The incidence and prognostic significance of acute kidney injury. Curr Opin Nephrol Hypertens. 2007;16:227–36.
7. Jeltsch M, Kaipainen A, Joukov V, et al. Hyperplasia of lymphatic vessels in VEGF-C transgenic mice. Science. 1997;276:1423–5.
8. Breiteneder-Geleff S, Soleiman A, Kowalski H, et al. Angiosarcomas express mixed endothelial phenotypes of blood and lymphatic capillaries: podoplanin as a specific marker for lymphatic endothelium. Am J Pathol. 1999;154:385–94.
9. Banerji S, Ni J, Wang SX, et al. LYVE-1, a new homologue of the CD44 glycoprotein, is a lymph-specific receptor for hyaluronan. J Cell Biol. 1999;144:789–801.
10. Wigle JT, Oliver G. Prox1 function is required for the development of the murine lymphatic system. Cell. 1999;98:769–78.
11. Maby-El Hajjami H, Petrova TV. Developmental and pathological lymphangiogenesis: from models to human disease. Histochem Cell Biol. 2008;130:1063–78.
12. Kim H, Kataru RP, Koh GY. Inflammation-associated lymphangiogenesis: a double-edged sword? J Clin Invest. 2014;124:936–42.

13. Seeger H, Bonani M, Segerer S. The role of lymphatics in renal inflammation. Nephrol Dial Transplant. 2012;27:2634–41.
14. Yazdani S, Navis G, Hillebrands JL, et al. Lymphangiogenesis in renal diseases: passive bystander or active participant? Expert Rev Mol Med. 2014;16:e15.
15. Dieterich LC, Seidel CD, Detmar M. Lymphatic vessels: new targets for the treatment of inflammatory diseases. Angiogenesis. 2014;17:359–71.
16. Tammela T, Alitalo K. Lymphangiogenesis: molecular mechanisms and future promise. Cell. 2010;140:460–76.
17. Kim H, Kataru RP, Koh GY. Regulation and implications of inflammatory lymphangiogenesis. Trends Immunol. 2012;33:350–6.
18. Alitalo K, Tammela T, Petrova TV. Lymphangiogenesis in development and human disease. Nature. 2005;438:946–53.
19. Ji RC. Lymphatic endothelial cells, inflammatory lymphangiogenesis, and prospective players. Curr Med Chem. 2007; 14:2359–68.
20. Hull TD, Kamal AI, Boddu R, et al. Heme oxygenase-1 regulates myeloid cell trafficking in AKI. J Am Soc Nephrol. 2015; 26:2139–51.
21. Zarjou A, Kim J, Traylor AM, et al. Paracrine effects of mesenchymal stem cells in cisplatin-induced renal injury require heme oxygenase-1. Am J Physiol Renal Physiol. 2011;300: F254–262.
22. Zarjou A, Bolisetty S, Joseph R, et al. Proximal tubule H-ferritin mediates iron trafficking in acute kidney injury. J Clin Invest. 2013;123:4423–34.
23. Sharp CN, Doll MA, Dupre TV, et al. Repeated administration of low-dose cisplatin in mice induces fibrosis. Am J Physiol Renal Physiol. 2016;310:F560–568.
24. Black LM, Lever JM, Traylor AM, et al. Divergent effects of AKI to CKD models on inflammation and fibrosis. Am J Physiol Renal Physiol. 2018;315:F1107–F1118.
25. Zhang MZ, Yao B, Yang S, et al. CSF-1 signaling mediates recovery from acute kidney injury. J Clin Invest. 2012; 122:4519–32.
26. Takahashi N, Boysen G, Li F, et al. Tandem mass spectrometry measurements of creatinine in mouse plasma and urine for determining glomerular filtration rate. Kidney Int. 2007; 71:266–71.
27. Zarjou A, Yang S, Abraham E, et al. Identification of a microRNA signature in renal fibrosis: role of miR-21. Am J Physiol Renal Physiol. 2011;301:F793–801.
28. Bolisetty S, Zarjou A, Hull TD, et al. Macrophage and epithelial cell H-ferritin expression regulates renal inflammation. Kidney Int. 2015;88:95–108.
29. Bolisetty S, Traylor AM, Kim J, et al. Heme oxygenase-1 inhibits renal tubular macroautophagy in acute kidney injury. J Am Soc Nephrol. 2010;21:1702–12.
30. Klotz L, Norman S, Vieira JM, et al. Cardiac lymphatics are heterogeneous in origin and respond to injury. Nature. 2015; 522:62–67.
31. Mitamura T, Higashiyama S, Taniguchi N, et al. Diphtheria toxin binds to the epidermal growth factor (EGF)-like domain of human heparin-binding EGF-like growth factor/diphtheria toxin receptor and inhibits specifically its mitogenic activity. J Biol Chem. 1995;270:1015–9.
32. Huang JL, Woolf AS, Kolatsi-Joannou M, et al. Vascular endothelial growth factor C for polycystic kidney diseases. J Am Soc Nephrol. 2016;27:69–77.
33. Cui Y, Liu K, Monzon-Medina ME, et al. Therapeutic lymphangiogenesis ameliorates established acute lung allograft rejection. J Clin Invest. 2015;125:4255–68.
34. Dietrich T, Bock F, Yuen D, et al. Cutting edge: lymphatic vessels, not blood vessels, primarily mediate immune rejections after transplantation. J Immunol. 2010;184:535–9.
35. Ling S, Qi C, Li W, et al. Crucial role of corneal lymphangiogenesis for allograft rejection in alkali-burned cornea bed. Clin Exp Ophthalmol. 2009;37:874–83.
36. Moriguchi P, Sannomiya P, Lara PF, et al. Lymphatic system changes in diabetes mellitus: role of insulin and hyperglycemia. Diabetes Metab Res Rev. 2005;21:150–7.
37. Yin N, Zhang N, Lal G, et al. Lymphangiogenesis is required for pancreatic islet inflammation and diabetes. PLoS One. 2011;6: e28023.
38. Sleeman JP, Thiele W. Tumor metastasis and the lymphatic vasculature. Int J Cancer. 2009;125:2747–56.
39. Stacker SA, Baldwin ME, Achen MG. The role of tumor lymphangiogenesis in metastatic spread. FASEB J. 2002;16:922–34.
40. Guo YC, Zhang M, Wang FX, et al. Macrophages regulate unilateral ureteral obstruction-induced renal lymphangiogenesis through C-C motif chemokine receptor 2-dependent phosphatidylinositol 3-kinase-AKT-mechanistic target of rapamycin signaling and hypoxia-inducible factor-1alpha/vascular endothelial growth factor-C expression. Am J Pathol. 2017; 187:1736–49.
41. Hasegawa S, Nakano T, Torisu K, et al. Vascular endothelial growth factor-C ameliorates renal interstitial fibrosis through lymphangiogenesis in mouse unilateral ureteral obstruction. Lab Invest. 2017;97:1439–52.
42. Lee AS, Lee JE, Jung YJ, et al. Vascular endothelial growth factor-C and -D are involved in lymphangiogenesis in mouse unilateral ureteral obstruction. Kidney Int. 2013;83:50–62.
43. Suzuki Y, Ito Y, Mizuno M, et al. Transforming growth factor-beta induces vascular endothelial growth factor-C expression leading to lymphangiogenesis in rat unilateral ureteral obstruction. Kidney Int. 2012;81:865–79.
44. Adair A, Mitchell DR, Kipari T, et al. Peritubular capillary rarefaction and lymphangiogenesis in chronic allograft failure. Transplantation. 2007;83:1542–50.
45. Palin NK, Savikko J, Koskinen PK. Sirolimus inhibits lymphangiogenesis in rat renal allografts, a novel mechanism to prevent chronic kidney allograft injury. Transpl Int. 2013;26:195–205.
46. Horiguchi A, Ito K, Sumitomo M, et al. Intratumoral lymphatics and lymphatic invasion are associated with tumor aggressiveness and poor prognosis in renal cell carcinoma. Urology. 2008;71:928–32.
47. Ozardili I, Guldur ME, Ciftci H, et al. Correlation between lymphangiogenesis and clinicopathological parameters in renal cell carcinoma. Singapore Med J. 2012;53:332–5.
48. Vaidya VS, Waikar SS, Ferguson MA, et al. Urinary biomarkers for sensitive and specific detection of acute kidney injury in humans. Clin Transl Sci. 2008;1:200–8.